

The hysteresis of the indices of solar activity and of the ionospheric indices in 11-yr cycles. The hysteresis of the stellar activity indices in the cyclic activity similar to the Sun

E.A.Bruevich ^a, G.V. Yakunina^a,
T.V. Kazachevskaya ^b, V.V. Katyushina ^b, A.A. Nusinov ^b

^aSternberg Astronomical Institute, MSU, Moscow, Russia

^bFedorov Institute of Applied Geophysics, Moscow, Russia

E-mail: ^ared-field@yandex.ru, ^bnusinov@ipg.geospace.ru

Abstract. The effects of hysteresis, which manifests itself in an ambiguous relationship between different indices for solar activity on the phases of rise and decline in the cycle, are analyzed for the indices of solar activity (which characterize the out coming radiation of the solar photosphere, chromosphere and corona) and also for the ionospheric indices. In the cycles 21 - 23 which are significantly different in amplitude, the effect of hysteresis manifests itself to a variable extent. The stars with the well-determined cycles were examined to detect the effect of hysteresis between the chromosphere's S-index CaII fluxes versus the photosphere's fluxes $F_{photosphere}$.

Key words. Sun: activity indices, solar-type stars: the HK- project, activity cycles.

1 Introduction

In solar and solar-terrestrial physics the phenomenon of hysteresis has long been known [1, 2, 3]. This effect manifests itself (for different levels of solar activity) in an ambiguous dependence of the radiation of the solar photosphere, chromosphere and corona, as well as indices characterizing the state of Earth's ionosphere. We have chosen to study the effect of the hysteresis in solar activity versus off the index $F_{10.7}$ (radio flux on the wave 10.7 cm – 2800 MHz).

The aim of this work is to study the variations of indices of activity during three solar cycles: (1) the changes in the values of the activity indices (AI - Activity Indices) depending on the solar activity level (i.e. versus the $F_{10.7}$

index), and (2) the analysis of the ambiguous dependence of the relationship of indices of activity versus $F_{10.7}$ on the rise and decline phases of the solar cycle.

For the monthly values of 7 activity indices AI we have determined the coefficients of the quadratic regression for the correlations with an $F_{10.7}$ index ($AI \leftrightarrow F_{10.7}$). Also we determined the coefficients of a quadratic regression for 5 daily values of indices of solar and ionospheric activity ($AI \leftrightarrow F_{10.7}$).

Thus a series of observations of the indices of the SSN, TSI and $F_{L\alpha}$ were analyzed for monthly and daily data.

We also analyzed the hysteresis of the solar-type stars (with a stable cycles of activity similar to the sun's cycles) between the radiation fluxes from their photospheres and chromospheres (in the lines H and K CaII) from the Mount Wilson HK-project and Lowell observatory data [4,5].

In this study we used the data of observations of $F_{10.7}$, SSN and other indices of solar and ionospheric activity from the archives of the NOAA National Geophysical Data Center and of the Solar-Geophysical Data Reports [6, 7].

2 The indices of activity at different phases of the 11-yr solar cycle. The hysteresis of their monthly values

We study the hysteresis of the solar and ionospheric indices, varying in the 11-yr cycle, depending on the overall level of solar activity which is defined by the value of $F_{10.7}$.

The solar radio microwave flux at wavelengths 10.7 cm $F_{10.7}$ has also the longest running series of observations started in 1947 in Ottawa, Canada and maintained to this day at Penticton site in British Columbia. This radio emission comes from high part of the chromosphere and low part of the corona. $F_{10.7}$ radio flux has two different sources: thermal bremsstrahlung (due to electrons radiating when changing direction by being deflected by other charged particles) and gyro-radiation (due to electrons radiating when changing direction by gyrating around magnetic fields lines). These mechanisms give rise to enhanced radiation when the temperature, density and magnetic fields are enhanced. So $F_{10.7}$ is a good measure of general solar activity. $F_{10.7}$ data are available at <http://radbelts.gsfc.nasa.gov>. The results

of measurements of the $F_{10.7}$ flux are expressed in units of solar flux (sfu): $1\text{sfu} = 10^{-22}\text{W} \cdot \text{m}^{-2} \cdot \text{Hz}^{-1}$.

SSN has the longest series of observations (monthly averaged values of the relative sunspot number are known since 1749, and annual averaged are known since 1700). The solar activity is currently studying with the help of other indices (simultaneously with the SSN), which are carrying the quantitative information about the general levels of activity in those areas of the solar atmosphere where they are formed.

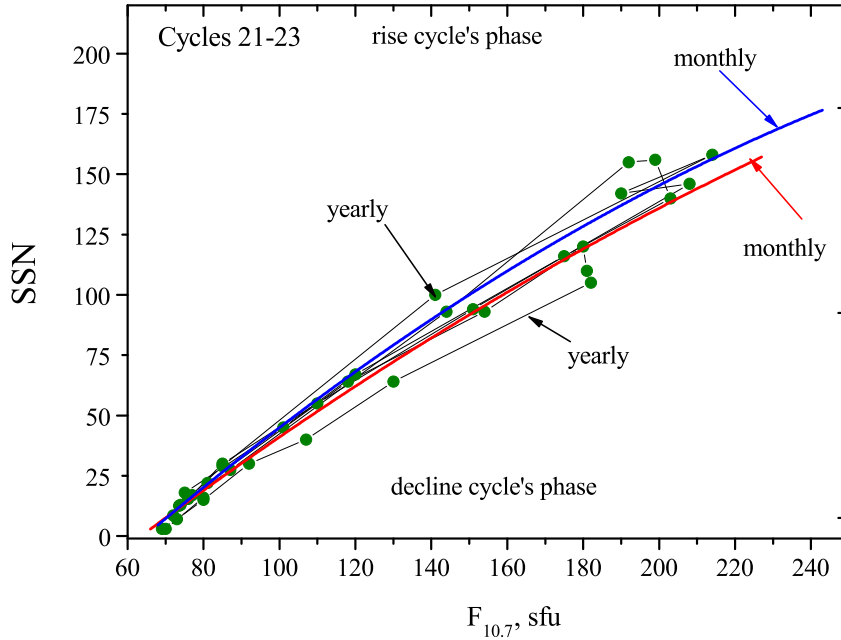


Figure 1: Monthly and annual averaged SSN depending on the monthly and annual averaged $F_{10.7}$.

The radiation flux in the ultraviolet $HL\alpha$ line (121.6 nm), $F_{L\alpha}$ – an important indicator of solar radiation, carrying the information of the chromosphere and bottom of the transition zone, [8].

Ultraviolet flux and X-rays represent a relatively small part in the total energy flux of solar radiation. This part of the spectrum is highly variable in time and strongly affects the upper atmosphere of the Earth causing ioniza-

tion and dissociation of atmospheric components, leading to the formation of the ionosphere. The activity index $F_{L\alpha}$ is measured in $10^{11} \text{ photon} \cdot \text{cm}^{-2} \cdot \text{sec}^{-1}$. Earlier the $F_{L\alpha}$ index was analyzed in our paper [9] on the basis of data obtained with SUPR devices which was installed on different Russian satellites.

The Mg II 280 nm is important solar activity indicator of radiation, derived from daily solar observations of the core-to-wing ratio of the Mg II doublet at 279,9 nm provides a good measure of the solar UV variability and can be used as a reliable proxy to model extreme UV (EUV) variability during the solar cycle [10]. The Mg II observation data were obtained from several satellite's (NOAA, ENVISAT) instruments. Comparison of the NOAA and ENVISAT Mg II index observation data shows that both the MgII indexes agree to within about 0,5%. We used both the NOAA and ENVISAT Mg II index observed data from Solar-Geophysical Data Bulletin [7] and [10]. In [11] it was shown an extremely good fit between the 30,4 nm emission (the main component of EUV-emission) and the NOAA Mg II index. In [11,12] it has been noted the close linear relationship between the Mg II index and total solar irradiance – TSI.

TSI is the solar irradiance is the total amount of solar energy at a given wavelength received at the top of the earth's atmosphere per unit time. When integrated over all wavelengths, this quantity is called the total solar irradiance (TSI) previously known as the solar constant. Regular monitoring of TSI has been carried out since 1978. We use the TSI data set from NGDC web site <http://www.ngdc.noaa.gov> and combined observational data from National Geophysical Data Center Solar and Terrestrial Physics [6]. The importance of UV/EUV influence to TSI variability (Active Sun/Quiet Sun) was pointed in [13]. There were indicated that up to 63,3 % of TSI variability is produced at wavelengths below 400 nm. Towards activity maxima the number of sunspots grows dramatically. But on average the TSI is increased by about 0,1% from minimum to maximum of activity cycle. This is due to the increase amounts of bright features, faculae and network elements on the solar surface. The total area of the solar surface covered by such features rises more strongly as the cycle progresses than the total area of dark sunspots. Some physics-based models have been developed with using the combined proxies describing sunspot darkening (sunspot number or areas) and facular brightening (facular areas, Ca II or Mg II indices), see [14].

We also analyzed rapid processes on the Sun: Counts of Flares – monthly counts of grouped solar flares (according [7] the term 'grouped' means obser-

vations of the same event by different sites were lumped together and counted as one) and Flare Index, summing the "total energy" emitted in the optical range in flares.

Earlier in [15] for the cycles 21 -23, we investigated the correlation between several solar activity indices and $F_{10.7}$. It turned out that the correlation coefficient depends on the phase of cycles of activity and its dependence on time is asymmetric for the rise and decline cycle's phases. This fact, along with detected shifts in time between the maximums of the values of indices of solar activity during one cycle indicates the existence of hysteresis of the solar indices.

We have analyzed the data for the rise and decline phases for three cycles of activity separately. The effect of hysteresis, with some differences in the values of the coefficients of the quadratic regression between the indices and $F_{10.7}$ was observed in each of these cycles.

It should be noted that according to the observations of indices of activity, in particular, SSN and TSI, the dependence of the ratio of the observed to the estimated AI in the regression ratios for the period 1950-1990 has changed markedly since 1990, previously this ratio was constant, see [16]. This has affected the values of coefficients of quadratic regressions between indices and $F_{10.7}$ in the cycle 23 compared to the cycles 21 and 22.

Figures 1 - 4 shows the monthly averaged values of SSN, $F_{L\alpha}$, MgII, TSI, Flare Index and $F_{530.3}$ depending on $F_{10.7}$ for the cycles 21 – 23. Due to significant scatter of data, it is advisable to compare the regression equations for each phase (rise and decline) separately. It was showed that to analyze the observation of solar indices is enough to use with polynomials of second order.

For the rise cycle's phases and the decline cycle's phases the solid lines are shown the quadratic regression lines. It is seen that the effect of hysteresis manifests itself in all activity indices and reach up to 10 - 15 % with the exception of the MgII index and the TSI, which have very small relative variations in the cycles of activity (Fig. 3a,b).

Fig. 1 also shows the dependence of the yearly averaged SSN from the yearly averaged $F_{10.7}$. It can be seen that the hysteresis value (the maximum relative deviation in the cycle) in yearly averaged case is increased to 20 %.

In Fig. 2 the solid lines are the lines of quadratic regression for the synthetic series of the $F_{L\alpha}$ (Composite Solar Lyman alpha the data from the Laboratory for Atmospheric and Space Physics at the University of Colorado, see http://lasp.colorado.edu/lisird/tss/composite_lyman_alpha.html).

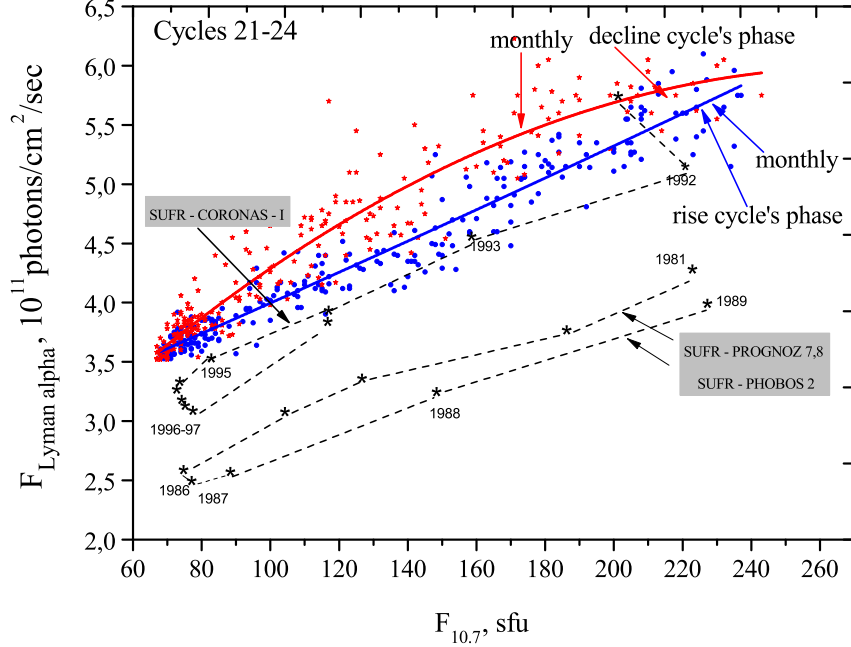


Figure 2: Monthly averaged $F_{L\alpha}$ depending on the monthly averaged $F_{10.7}$

The dashed lines refer to the yearly averaged data over the year of observations of SUFR (PHOBOS 2, PROGNOZ 7,8, CORONAS) for the cycles 21 and 22, see [9].

In Fig. 3a,b the solid lines are the lines of quadratic regressions of monthly averaged values of the MgII and the TSI in the cycles 21-23. In Fig. 3b we also present the 365-day moving averages of the TSI for the rise and decline phases of the cycle 21. We can see that the effect of hysteresis in the case of the 365-day moving averages is more pronounced.

Fig. 4a,b shows that the indices associated with the rapidly varying solar activity are characterized by a hysteresis value of about 10 – 20 %.

The quadratic regressions which are shown in Fig. 1 - 4, are described by equation (1):

$$AI = A + C1 \cdot F_{10.7} + C2 \cdot F_{10.7}^2. \quad (1)$$

here AI is solar activity index,

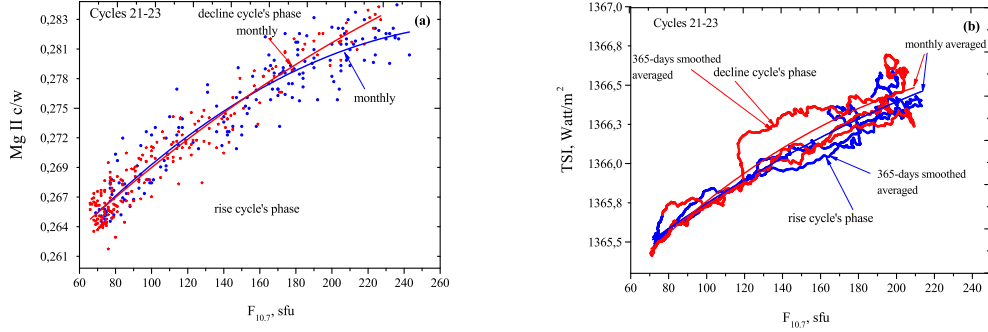


Figure 3: The MgII (a) monthly averaged values and the TSI (b) monthly averaged values versus the monthly averaged $F_{10.7}$

A is the intercept of polinomial regression,
 C1 and C2 are the coefficients of polinomial regression. These coefficients are presented in the Table 1.

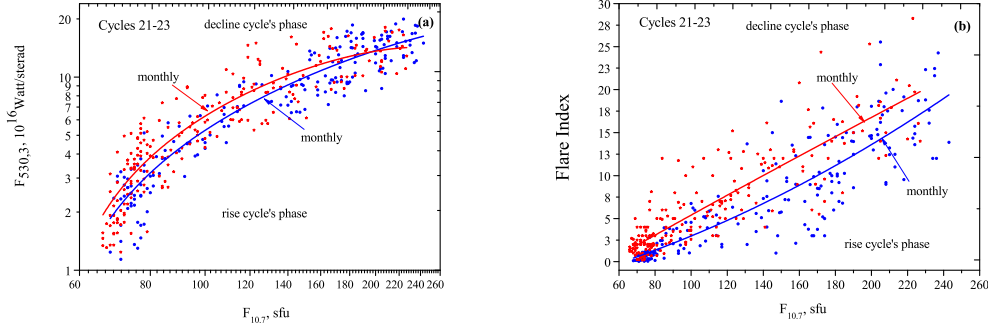


Figure 4: The monthly averaged values of the Flare Index (a) and radiation flux $F_{530.3}$ (b) versus the monthly averaged $F_{10.7}$

In the Table 1 the regression coefficients A, C1 and C2 are indicated for the rise (R) and decline (D) phases of solar cycle. σ_A , σ_{C1} , σ_{C2} are the standard deviations of the values of the regression coefficients. The statistical estimates show that the regression coefficients for the phases of rise and decline in the cycles of activity vary with the level of significance which is equal to $\alpha=0.05$.

Table 1: The coefficients of the quadratic regression for monthly averaged values of the activity indices AI in the cycles 21, 22 and 23 in the phases of rise (R) and decline (D)

AI \leftrightarrow $F_{10.7}$	A	C1	C2	σ_A	σ_{C1}	σ_{C2}
MgII \leftrightarrow $F_{10.7,R}$	0.252	2.1E-4	1.9E-5	0.0014	3.7E-7	6.7E-8
MgII \leftrightarrow $F_{10.7,D}$	0.254	1.7E-4	1.8E-5	0.0009	1.9E-7	5.6E-8
$F_{L\alpha} \leftrightarrow F_{10.7,R}$	2.126	0.022	-2.7E-5	0.16	0.0025	8.5E-6
$F_{L\alpha} \leftrightarrow F_{10.7,D}$	1.543	0.035	-7.4E-5	0.18	0.0028	9.9E-6
SSN \leftrightarrow $F_{10.7,R}$	-87.7	1.41	-8.8E-4	11.9	0.198	6.7E-8
SSN \leftrightarrow $F_{10.7,D}$	-79.7	1.34	-0.001	6.2	0.103	5.6E-8
Count F1 \leftrightarrow $F_{10.7,R}$	-356.5	6.8	-0.01	40.17	0.68	4.7E-3
Count F1 \leftrightarrow $F_{10.7,D}$	-206.2	3.21	0.006	32.48	0.35	4.9E-4
TSI \leftrightarrow $F_{10.7,R}$	1364.3	0.019	-4.5E-5	0.184	0.003	8.7E-6
TSI \leftrightarrow $F_{10.7,D}$	1364.5	0.015	-2.6E-5	0.161	0.002	9.2E-6

3 Hysteresis of daily values of solar and ionospheric activity indices in different phases of the 11-year cycle.

Earlier in this paper we have identified effects of hysteresis for monthly values. It is of interest to perform well as the average daily values of the indices. The investigated indices of the activity of the Sun AI are described by the same quadratic regression (1). The regression coefficients for the daily averaged values are presented in the Table 2, all the symbols in this Table 2 are corresponded to the designations of Table 1.

Fig. 5 shows that the daily SSN data are characterized by a large scatter of values, as in the paper [3]. Solid lines indicate the regression line for the daily data of SSN observations, while the dashed show the monthly data. It is seen that for daily values, the effect of hysteresis is more pronounced.

In Fig. 6a,b we also see the large scatter of the daily values of indices. The solid lines show the regression line for the daily data, the dashed lines in Fig. 6a show the regression line for monthly data.

It is known that the F2-region of ionosphere is formed under the influence of ionizing solar EUV radiation in the thermosphere of the Earth, which depends on the level of solar and geomagnetic activity. One of the manifestations of the nonlinear relationship between the foF2 the critical frequency

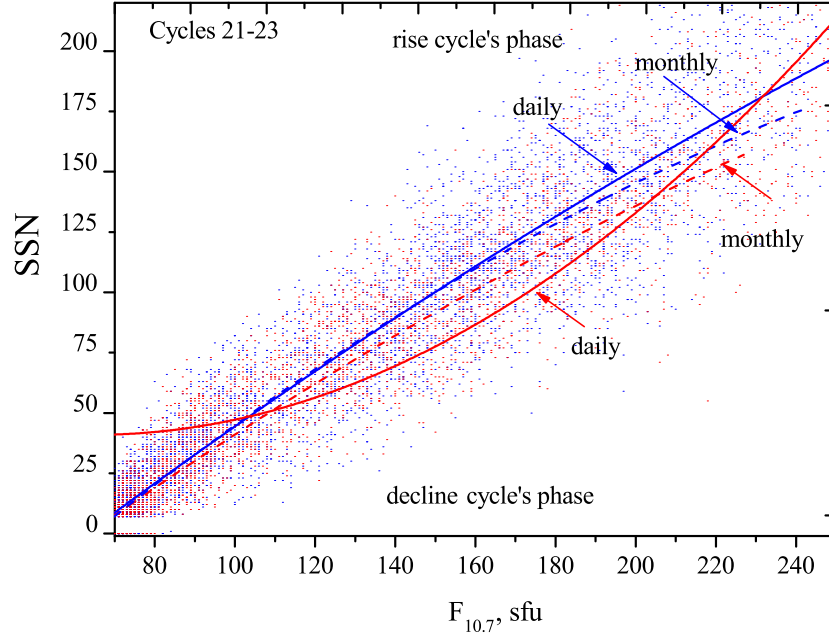


Figure 5: The daily values of the SSN depending on the daily averaged $F_{10.7}$

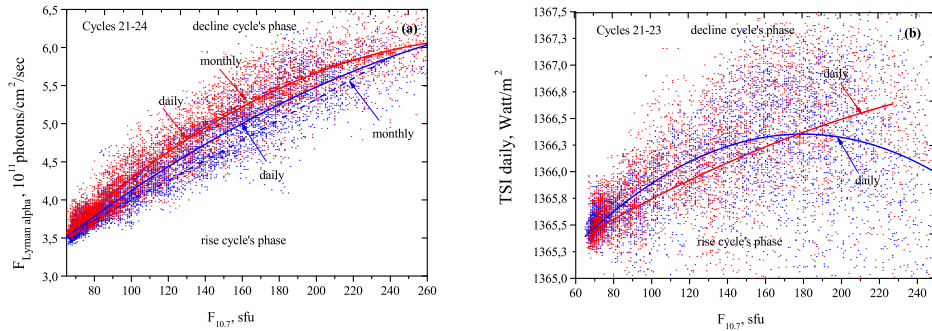


Figure 6: The daily values of the $F_{L\alpha}$ (a) and of the TSI (b) depending on the daily averaged $F_{10.7}$

of the F2 layer and solar activity indices AI is the effect of the hysteresis of foF2 variations in the 11 - yr cycle, [17].

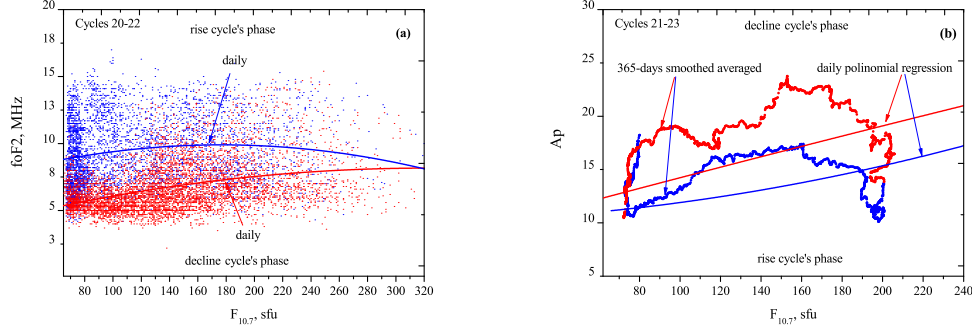


Figure 7: The daily values of the ionospheric indices $foF2$ (a) and of the A_p (b) depending on the daily averaged $F_{10.7}$

Regular daily variations of the magnetic fields are created mainly by changes of currents in the ionosphere due to the change of illumination of the ionosphere by the Sun during the day. Irregular variations of the magnetic field generated due to the flow of solar plasma (solar wind) which is acted on the Earth's magnetosphere and are associated with the flare activity of the Sun, changes in the magnetosphere, and the interaction of the magnetosphere and ionosphere. You must take into account that the ionospheric activity indices dependent on the level of solar activity in a complex manner: as in the case of the solar indices is the place ambiguous dependence on $F_{10.7}$.

In Fig. 7 the solid lines show the regression line for the daily data of the ionospheric indices $fo2$ and A_p . It is seen that ionospheric indices weakly depend on the level of solar activity. The effect of hysteresis on the rise and decline cycle's phases is expressed greatly. Fig. 7b presents a 365-day moving averages of A_p index for 21 cycles. The effect of hysteresis in the case of the 365-day moving averages is more pronounced.

4 The effects of hysteresis in the cyclic activity of stars in HK project

At the Mount Wilson Observatory in the framework of the HK project the regular observations of the star - analogues of the Sun were conducted from 1965 to the present. For the stars which were selected for the HK-project program it was defined by a comprehensive index the Mount Wilson S-index

Table 2: The coefficients of the quadratic regression for daily averaged values of the activity indices AI in the cycles 21, 22 and 23 in the phases of rise (R) and decline (D)

AI \leftrightarrow $F_{10.7}$	A	C1	C2	σ_A	σ_{C1}	σ_{C2}
SSN \leftrightarrow $F_{10.7,R}$	-81.2	1.35	-9.4E-4	1.71	0.024	7.9E-5
SSN \leftrightarrow $F_{10.7,D}$	61.86	-0.65	0.005	0.85	0.017	7.3E-5
TSI \leftrightarrow $F_{10.7,R}$	1364.0	0.026	-7.3E-5	0.04	5.52E-4	1.7E-6
TSI \leftrightarrow $F_{10.7,D}$	1364.7	0.013	-1.7E-5	-6.6E-4	9.5E-6	3.2E-8
$F_{L\alpha}$ \leftrightarrow $F_{10.7,R}$	2.21	0.022	-2.7E-5	0.017	0.00025	9.2E-7
$F_{L\alpha}$ \leftrightarrow $F_{10.7,D}$	1.97	0.028	-4.6E-5	0.02	0.00027	8.9E-7
foF2 \leftrightarrow $F_{10.7,R}$	7.19	0.031	-8.7E-5	0.24	0.0037	1.3E-5
foF2 \leftrightarrow $F_{10.7,D}$	3.77	0.027	-4.3E-5	0.16	0.0022	6.8E-6
Ap \leftrightarrow $F_{10.7,R}$	10.24	0.008	8.9E-5	1.21	0.002	6.3E-6
Ap \leftrightarrow $F_{10.7,D}$	9.18	0.052	-9.4E-6	1.32	0.018	2.2E-6

(S-index Call) - subsequently, the most important standard for characterizing the activity of the atmospheres of stars in the optical spectral range, see [4]. This program was specifically designed to study the cyclic activity in F, G and K stars of the solar type. In the result of long-term observations (over 40 years) it was significantly detected the activity cycles for about 50 stars. It was found that on the surface of stars, there are inhomogeneities that exist and vary over multiple periods of rotation of the star around its axis. In addition, the evolution of the rotation periods of the stars clearly indicates the existence of differential rotations of the star, similar to the differential rotations of the Sun, [4, 5]. The evolution of active regions on the star on a time scale of about 10 years determines the cyclic activity similar to the Sun.

For 111 HK-project stars the, periodograms were computed for each stellar record in order to search for activity cycles, [4]. The significance of the height of the tallest peak of the periodogram was estimated by the false alarm probability (FAP) function. The stars with cycles were classified as follows: if for the calculated $P_{cyc} \pm \Delta P$ the FAP function $\leq 10^{-9}$ then this star is of "Excellent" class (P_{cyc} is the period of the cycle). If $10^{-9} \leq FAP \leq 10^{-5}$ then this star is of "Good" class. If $10^{-5} \leq FAP \leq 10^{-2}$ then this star is of "Fair" class. If $10^{-2} \leq FAP \leq 10^{-1}$ then this star is of "Poor" class.

At the Lowell and Fairborn Observatories the photometric observations of the (Stromgren b, y photometry) was carried out in parallel with observations

of the S-index Call at the Observatory Mount Wilson for the 32 stars from the same sample in a period of 13-20 years [5]. In most cases, the observed link between fluxes in the chromospheres and photospheres of the stars: for one samle of stars there is positive correlation between these fluxes (as in the case of the Sun), for the others - the negative correlation.

In [18] it was made the analysis of the data on variability of optical radiation for the stars of the HK-project and on variability of optical radiation the stars observed at the Crimean astrophysical Observatory. The close relationship between spotting of the stars with very different levels of activity and power of their x-ray emission was found [18,19]. The analysis of atmospheric activity of solar-type stars using observations, including HK-project and three broad program of searches for planets, in which it were determined the magnitudes of the Call S-index for thousands of stars showed that stars of the HK-project are the closest to the Sun on the level of chromospheric, coronal radiation and the cyclical activity [19, 20, 21].

We chose 4 star of the HK-project with the highest quality of cyclical activity of "Excellent" class. This class corresponds to class calculated for them according to values of FAP [Bal]. These stars are: HD 103095 (a); HD 160346 (b), HD 81809 (C); HD 152391 (d). These stars belong to spectral classes G and K. For these stars in [5] the graphs of simultaneous observations chromospheric Mount Wilson S-index and photometric observations at Lowell Observatory are presented. The star HD 103095 and HD 160346 are characterized by a cyclic activity with periods of about 7 years, we studied 3 full cycle of activity. For the star HD 81809 and HD 152391 with longer cycles we studied 2 full cycles of activity only. Using the graphical dependencies from [4,5], we created a dataset for these 4 stars (which represent the average value for 3 months of observations). So we have made a necessary for our study the couple of indices of chromospheric and photospheric activity: S-index Call versus $F_{photosphere}$ separately for the phases of rise and phases of decline of star's activity cycles.

In Fig. 8 we present the averaged over 3 months of observations the S-index Call values depending on the $F_{photosphere}$ values. Solid lines indicate regression curves for the rise cycle's phase and decline cycle's phase of stellar cycles chromospheres activity.

The data of observations of stellar indices are also being explored with polynomials of second order. It is seen that for the selected stars with the cyclicity of the class "Excellent" there is a hysteresis effect for the analyzed pairs of indices characterizing chromosphere and photospheric activity.

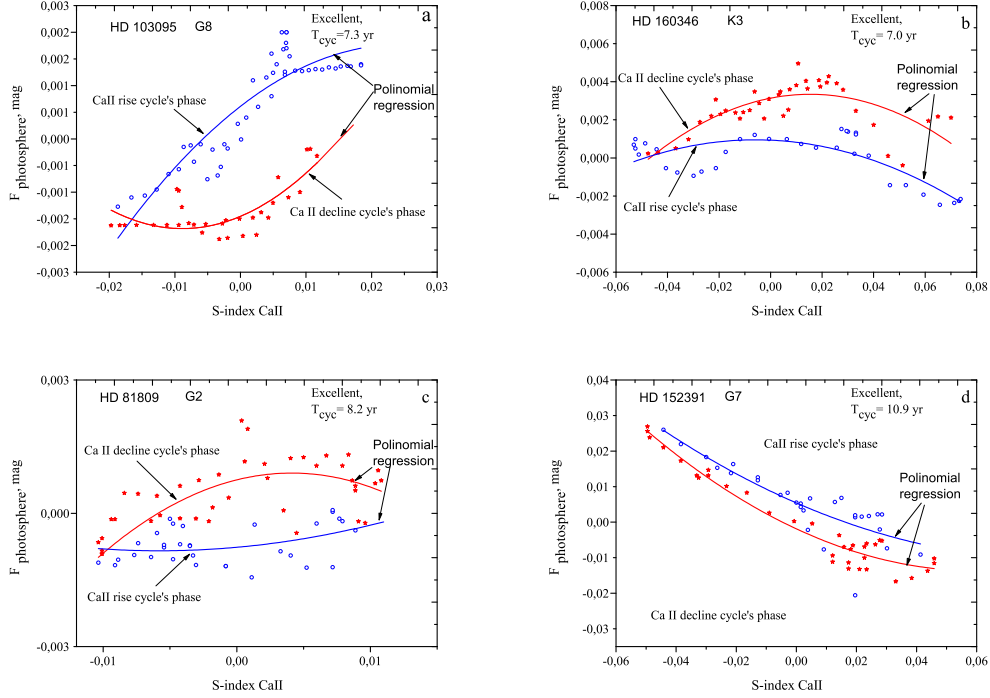


Figure 8: The effect of hysteresis in stars with activity cycles between chromospheres S-index CaII and the flow of radiation from the photosphere $F_{photosphere}$: HD 103095 (a); HD 160346 (b), HD 81809 (c); HD 152391 (d). The hollow circles correspond to the phases of rise of the cycles for the S CaII index, the asterisks correspond to the phases of decline of the cycles.

Phases of rise and decline in the cycles of activity are determined by increase and decrease of a universal index of activity of the chromosphere, the S-index Call. Note that with the increase in the activity of the chromosphere, photosphere activity does not always increase (as in the case of the Sun and stars HD 103095 and HD 81809 in Fig. 8a and 8c) and may remain approximately constant or decrease, see Fig. 8b (HD 160346) and 8d (HD 152391).

5 Discussion

We can see from the above consideration that the hysteresis effects exist for the various manifestations of solar activity from variations in the short wavelength range to the optical and radio bands, and are found in the manifestations of ionospheric and geomagnetic activity, and solar-type stars with detected cycles of activity.

For individual activity indices ($F_{L\alpha}$, foF2, $F_{10.7}$) the effect of hysteresis can be explained using the two-component model, [22]. According to the two-component model the radiation flux I_λ in the line is equal to:

$$I_\lambda = B0 + B1 \cdot (F_B - 60)^{2/3} + B2 \cdot (F_{10.7} - F_B)^{2/3}. \quad (2)$$

where F_B is the background radiation flux from the undisturbed surface of the solar disk (with no active regions). Background radiation F_B on the wave of 10.7 cm varies in a cycle of solar activity from 60 to 120 sfu, [23].

The analysis of cyclic variations in $F_{10.7}$ showed that, on average, an empirical regression of the ratio of radio flux $F_{10.7} = a + b \cdot F_B$ is performed. Here the coefficients a and b characterize the contribution from the two components of the model and change (1) at different phases of the activity cycles, and (2) from cycle to cycle, [22].

This fact determines the uneven relative decline and the increase of flows for the studied pairs of indices of activity at different phases of the solar cycle, which leads to hysteresis. The flow in weak cycles is determined mainly by the background radiation flux, and in strong cycles are relatively more important becomes the contribution from active regions of hysteresis effects should be more pronounced in stronger cycles, see [22]. A possible mechanism for the emergence of hysteresis at the present time is explained as a result of the asymmetry of solar Dynamo in the different phases of magnetic cycles, [24, 25].

6 Conclusions

The effect of hysteresis is typical not only for pairs of activity indices in 11-yr solar cycles, but for the stars of the HK- project with detected the stable cycles of activity similar to the Sun. Hysteresis is a real delay in the onset of the maximum and decline phase of solar and stellar activity and is an

important key in the search for physical processes responsible for changing radiation at different wavelengths.

The effect of hysteresis is apparently a common property of astronomical systems, which are characterized by different manifestations of the cyclic activity associated with the time evolution of magnetic fields. The hysteresis of foF2 is exist due to the ionospheric response to variations in solar activity, in particular, we can see the hysteresis in EUV radiation and hysteresis of the geomagnetic activity index AP. All this hysteresis effects is due to the hysteresis of the solar Dynamo.

For pairs of indices of solar activity and solar-type stars activity the effect of hysteresis appears in different ways. The curves of a hysteresis on the rise and decline cycle's phases vary from one cycle to another.

References

- [1] Watanabe, K., and Hinteregger, H. E., 1962, *J. Geophys. Res.*, **67**, 999-1006.
- [2] Ching, B.K., and Chiu, Y. T., 1973, *J. Atmos. Terr. Physics*, **35**, 1615-1630.
- [3] Bachmann, K. T., and White, O. R., 1994, *Solar Physics*, **150**, 347-357.
- [4] Baliunas, S. L., Donahue, R. A. et al., 1995, *Astrophys. J.*, **734**, 269-285.
- [5] Lockwood, G. W., Skif, B. A., Radick, R. R., Baliunas, S. L., Donahue, R. A., Soon, W., 2007, *Astrophys. J. Suppl.*, **171**, 260-290.
- [6] National Geophysical Data Center Solar and Terrestrial Physics. 2016, <http://www.ngdc.noaa.gov/stp/solar/solardataservices.html>.
- [7] Solar-Geophysical Data Reports. 54 Years of Space Weather Data, 2009, <http://www.ngdc.noaa.gov/stp/solar/sgd.html>.
- [8] Nusinov, A. A., Katyushina, V.V., 1994, *Solar Physics*, **152**, 201-206.
- [9] Kazachevskaya, T. V., and Katyushina, V.V., 2000, *Phys. Chem. Earth*, *25*, 425-427.

- [10] Skupin, J., Weber, M., Bovensmann, H., Burrows J.P. 2005, in *The 2004 Envisat and ERS Symposium (ESA SP-572)*, 6-10 September 2004, Salzburg, Austria. (eds) H. Lacoste, 55-59.
- [11] Viereck, R., Puga, L., McMullin, D., Judge, D., Weber, M. and Tobiska, K. 2001, *J. Geophys. Res.*, **28(7)**, 1343-1353.
- [12] Floyd, L., Newmark, J., Cook, J., Herring, L. and McMullin, D. 2005, *Journal of Atmospheric and Solar-Terrestrial Physics*, **67**, 3-12.
- [13] Krivova, N.A., and Solaki, S.K. 2008, *J. Astrophys. Astron.*, **29**, 151-161.
- [14] Krivova, N.A., Solanki, S.K., Fligge, M., Unruh, Y.C. 2003, *Astron. and Astrophys.*, **399**, L1.
- [15] Bruevich, E.A., Bruevich, V.V., and Yakunina, G.V., 2014, *J. Astrophys. Astron.*, **35**, 1-15.
- [16] Bruevich, E.A., and Yakunina, G.V., 2015, *Geomagnetism and Aeronomy*, **55**, 1060-1065.
- [17] Mikhailov, A.V., Mikhailov, V.V., 1993, *Geomagnetism and Aeronomy*, **33**, 89-95.
- [18] Bruevich, E.A., Alekseev, I.Yu. 2007, *Astrophysics*, **50**, 187.
- [19] Bruevich, E.A., Bruevich, V.V., Shimanovskaya, E.V., 2016, *Astrophysics*, **59**, 101-113.
- [20] Bruevich E.A., Kononovich E.V. 2011, *Moscow University Physics Bulletin*, **66**, 72-77.
- [21] Bruevich, E.A., and Yakunina, G.V., 2015, *Moscow University Physics Bulletin*, **70**, 282-290.
- [22] Nusinov, A. A., 1996, *Radiophysics and Quantum Electronics*, 1996, **39**, 830-832.
- [23] Bruevich, E.A., Nusinov, A.A., 1984, *Geomagnetism and Aeronomy*, 1984, **70**, 581-585.

- [24] Kitchatinov, L. L., Olemskoy, S. V., 2010, *Astronomy Letters*, **36**, 292-296.
- [25] Pipin, V.V., Kosovichev, A.G., 2015, *Astrophys. J.*, 2015, **813**, 134-145.